Improved confidence in IVIM diffusion metrics from 'post-navigator' registration of individual coronal signal average images in abdominal DW-MRI

Neil P Jerome[1], Matthew R Orton[1], James d'Arcy[1], Dow-Mu Koh[2], David J Collins[1], and Martin O Leach[1]

[1]*CR-UK and EPSRC Cancer Imaging Centre, The Institute of Cancer Research, Sutton, Surrey, United Kingdom,* [2]*Department of Radiology, Royal Marsden Hospital, Sutton, Surrey, United Kingdom*

Introduction: Respiratory motion commonly confounds abdominal diffusion-weighted (DW) MRI, producing blurring in the images as a function of the number of b-values and signal averages acquired. Strategies to minimise respiratory motion can adversely affect scan efficiency (e.g. navigator-triggering) or patient comfort (e.g. breath-hold) without necessarily improving diffusion parameter estimation (1), and rely on potentially invalid assumptions about breathing patterns and consistency. Coronal imaging brings respiratory motion, predominantly head-foot for the abdomen, into the imaging plane; recording each signal average and diffusion gradient direction as a separate series allows for post-acquisition registration of each image, removing the largest source of blurring present with no cost reflected in imaging time. Acquiring separate images also allows deeper interrogation of the data, and potentially the ability to cull aberrant images that may show through-plane respiratory motion or other effects. We apply this technique with the IVIM model of DW-MRI and show a resulting decrease in model fitting residuals, indicating a greater confidence in fitted diffusion parameters as well as visually sharper images.

Method: This study was approved by the institutional review board; ten healthy volunteers were recruited and consented; all imaging was performed on a MAGNETOM Avanto 1.5T scanner (Siemens AG, Healthcare Sector, Erlangen, Germany). Coronal slices were taken to cover the kidneys, with parameters: 2D EPI sequence with bipolar diffusion weighting, TR 4000 ms, TE 72 ms, voxel size 1.5 mm^2 in-plane, 16 contiguous 5mm slices, 128 x 128 matrix with GRAPPA factor 2, interpolated to 256 x 256, with nine b-values (0, 20, 40, 60, 80, 100, 250, 500, 750 s/mm^2) in orthogonal directions and trace images calculated. Multiple signal average series were taken (5 to 6 images), for an approximate acquisition time of 10 minutes. Following acquisition, individual images for each series and b-value were registered manually (focusing on the each kidney in turn) to the mean b=0 image by use of pixel-wise shifting. Where the required shift magnitude was found to be greater than (mean + 2×s.d.), the image was labeled an outlier. Fitting of the IVIM diffusion model to unregistered images, registered images, and registered images without outliers, was performed with all b-values using a Bayesian approach in proprietary software (ADEPT, ICR, UK). ROIs for whole kidney, renal cortex, and renal medulla were drawn on the registered images, and resulting diffusion parameters are reported as mean ± s.d., were compared using a paired t-test with significance level 0.05.

Figure 1: Mean b=0 images before (left) and after (right) voxel-wise shifting registration; arrows indicate blurred boundaries.

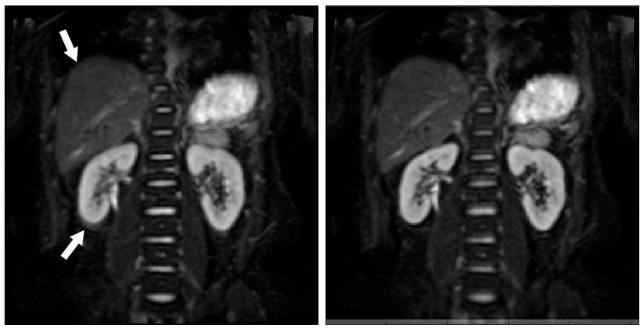

Figure 2: Ladder plots for residual sum-of squares from IVIM model in kidney ROI. Black line = mean (n=17).

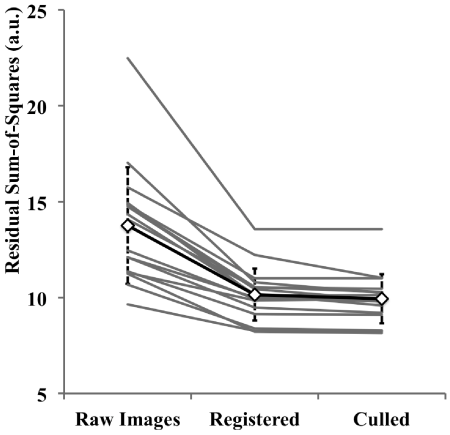

Results: Manual registration of the all individual images yields a visually sharper image for the kidney considered (representative mean b=0 images displayed in **figure 1**); IVIM diffusion parameters for the cohort (mean ± sd) are reported in **table 1** for unprocessed images, registered images, and registered with culling of outliers. For the ROIs derived from the entire kidney, there is only a small decrease in perfusion fraction (15.9 to 15.3%, p=0.043); the flow-associated parameter fD* is significantly reduced in all ROIs, with all other sub-region parameters unchanged. The normalised residual sum-of-squares, a proxy for the confidence of the fitting, is significantly reduced with registration in all ROIs (**figure 2**). The definition and exclusion of outliers as applied here appears to convey a further decrease in residuals, significant when compared to both unregistered and registered images.

Discussion: Sufficient signal averaging is used to give robust ROI DWI statistics, and registration/culling of individual images, practiced for diffusion tensor imaging in the brain (2), yields IVIM parameters with greater confidence as indicated by the reduced residuals from model fitting. While the comparatively large range of respiratory motion (including deformations and through-plane motion) in abdominal imaging precludes the same level of analysis as diffusion tensor imaging (DTI), simple registration in-plane can be used to largely account for the observed head-foot motion and improve image appearance. While complex registration schemes may be more rigorous, whole-pixel increment translation is attractively simple, does not interpolate raw data, and offers the lion's share of blurring reduction whilst being fast enough to automate in the normal workflow. The improved confidence offered by voxel-wise shifting may offer greater sensitivity of DWI measurements to small changes arising from disease progression or treatment response, and potentially facilitate a move from ROI statistics to interrogation of pixel-maps. With full access to individual images, other criteria for identifying and culling outliers from the dataset, not yet explored, may yield further improvements.

Table 1: IVIM statistics for pre- and post- registration, and with outlier culling. **Bold** p<0.05 to raw images, *italic* p<0.05 to registered. ROI sizes: kidney (1986 ± 193), renal cortex (118 ± 22), and renal medulla (106 ± 27) voxels. Results are given as mean ± s.d.

	Whole Kidney			Renal Cortex			Renal Medulla		
	Raw	Registered	Culled	Raw	Registered	Culled	Raw	Registered	Culled
f (%)	15.9 ± 3.6	**15.3 ± 3.7**	15.3 ± 3.8	13.4 ± 4.9	13.2 ± 5.0	13.2 ± 5.0	16.9 ± 7.3	14.7 ± 6.9	14.8 ± 6.6
D (10^{-5} mm^2s^{-1})	202 ± 10	202 ± 11	202 ± 11	205 ± 12	205 ± 14	203 ± 13	193 ± 13	193 ± 12	192 ± 12
D* (10^{-2} mm^2s^{-1})	4.3 ± 0.7	3.9 ± 0.7	3.9 ± 0.8	3.5 ± 1.0	3.1 ± 1.1	3.0 ± 1.1	4.6 ± 1.4	4.2 ± 1.3	4.2 ± 1.3
fD* (10^{-4} mm^2s^{-1})	53.0 ± 10.8	**44.2 ± 7.4**	**43.7 ± 8.9**	41.1 ± 14.0	**32.6 ± 4.8**	**32.1 ± 5.6**	71.8 ± 41.8	**53.4 ± 34.3**	**54.2 ± 34.5**
Residuals (a.u.)	13.8 ± 3.0	**10.2 ± 1.4**	***9.9 ± 1.3***	13.2 ± 4.2	**9.5 ± 1.0**	***9.3 ± 0.9***	15.4 ± 4.3	**11.0 ± 2.3**	***10.8 ± 2.2***

Acknowledgements: This work was funded by CR-UK grant number C7273. We also acknowledge the support received for the CRUK and EPSRC Cancer Imaging Centre in association with the MRC and Department of Health (England) (grants C1060/A10334 and C16412/A6269) and NHS funding to the NIHR Biomedical Research Centre and the NIHR Clinical Research Facility. We also thank Dr. Thorsten Feiweier at Siemens AG, Healthcare Sector for providing the prototype DWI package. **References:** (1) Jerome, NP; Orton, M; d'Arcy, J; Collins, DJ; Koh, D-M; Leach, MO, *Proc. ISMRM 2012*, Abstract 1316. (2) Chang L-C, Jones DK, Pierpaoli C., *Magnetic Resonance in Medicine,* 2005;53, 1088